Accepted Manuscript

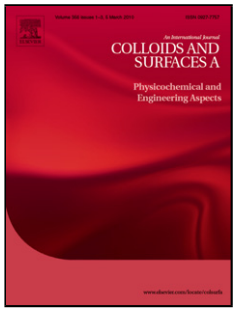

Title: Iron Oxide Nanoparticles (IONPs) with potential applications in plasmid DNA isolation

Authors: J.R Sosa-Acosta, J.A. Silva, L. Fernández-Izquierdo, S. Díaz-Castañón, M. Ortiz, J.C. Zuaznabar-Gardona, A.M. Díaz-García

PII: S0927-7757(18)30151-1
DOI: https://doi.org/10.1016/j.colsurfa.2018.02.062
Reference: COLSUA 22314

To appear in: *Colloids and Surfaces A: Physicochem. Eng. Aspects*

Received date: 15-12-2017
Revised date: 23-2-2018
Accepted date: 25-2-2018

Please cite this article as: Sosa-Acosta JR, Silva JA, Fernández-Izquierdo L, Díaz-Castañón S, Ortiz M, Zuaznabar-Gardona JC, Díaz-García AM, Iron Oxide Nanoparticles (IONPs) with potential applications in plasmid DNA isolation, *Colloids and Surfaces A: Physicochemical and Engineering Aspects* (2010), https://doi.org/10.1016/j.colsurfa.2018.02.062

Title: Iron Oxide Nanoparticles (IONPs) with potential applications in plasmid DNA isolation

Author names and affiliations: Sosa-Acosta J.R. [(1)], Silva J.A. [(2)], Fernández-Izquierdo L. [(3)], Díaz-Castañón S. [(4)], Ortiz M. [(5)], Zuaznabar-Gardona J. C. [(5)], Díaz-García A.M. [*(6)]

(1): Physical-Chemistry Department, Bioinorganic Laboratory (LBI), University of Havana, Cuba
(2): Center for Genetic Engineering and Biotechnology (CIGB), Havana, Cuba
(3): Center for Advanced Studies of Cuba (CEAC) and Pontifical Catholic University of Chile, Chile
(4): Advanced Materials, Division, IPICYT, Mexico
(5): Nanobiotechnology & Bioanalysis Group, Departament d' Enginyeria Química, Universitat Rovira i Virgili, Tarragona, Spain
(6): Inorganic and General Chemistry Department, Bioinorganic Laboratory (LBI), University of Havana, Cuba

Corresponding author*: Díaz-García A.M. adg@fq.uh.cu or adg1959@gmail.com , Zapata and G, Vedado, Plaza, Havana, Cuba. ZIP: 10400

Graphical abstract

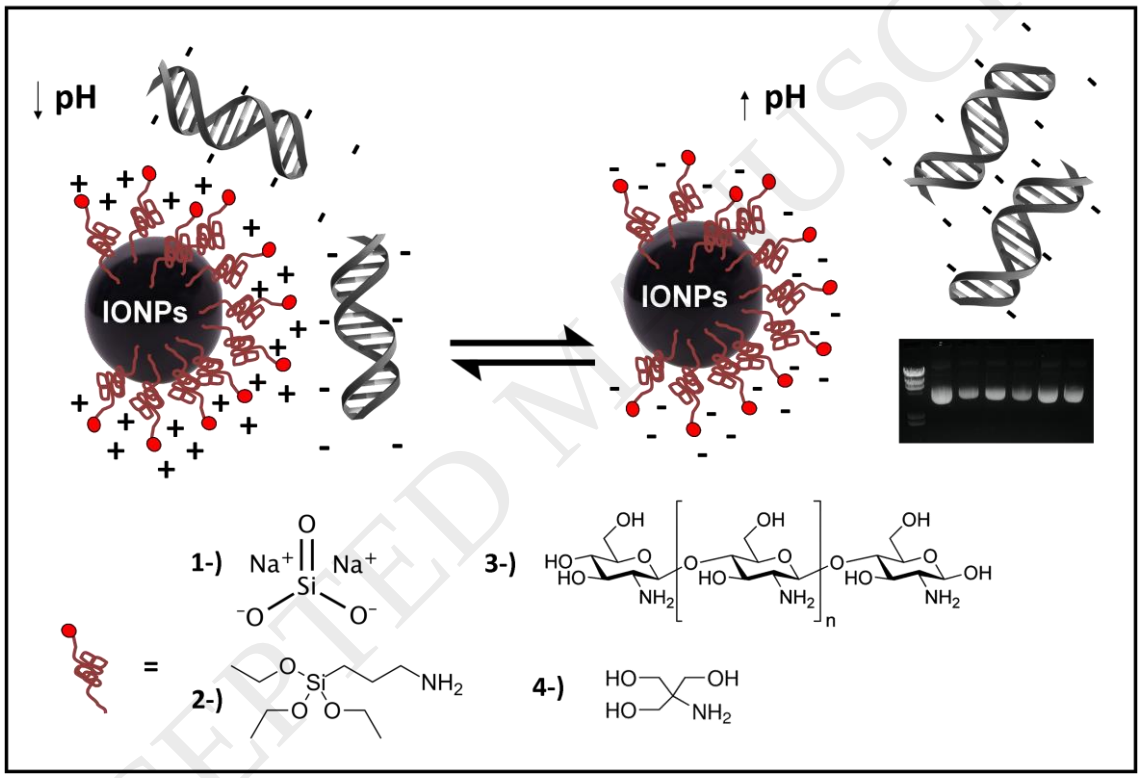

Abstract: DNA extraction and purification is considered a critical step in different biomedical applications such as genetic therapy and clinical diagnosis. This research describes the synthesis and characterization of functionalized IONPs with potential applications in plasmid DNA isolation. IONPs were synthesized by the chemical coprecipitation method followed by a post-synthesis functionalization using silica and (3-aminopropyl)triethoxysilane (APTES). A second functionalization strategy was carried out by an *in situ* coprecipitation of Fe(II) and Fe(III) ions in presence of chitosan and tris(hydroxymethyl)aminomethane (Tris). IONPs characterization by X-Ray diffraction (XRD) confirmed the synthesis of inverse-spinel magnetite like nanoparticles. In addition, infrared spectroscopy allowed to identify the hydroxyl, silanol and amino functional groups on the surface of the nanoparticles. Transmission electron microscopy measurements revealed IONPs with an average particle size under 13 nm. According to saturation and remanence magnetization values, all samples were suitable for bioseparation studies using magnetic manipulation. Preliminary separation assays with oligodeoxynucleotides (ODN) and plasmid DNA (pDNA) were carried out. Furthermore, biomolecular integrity of ODN and pDNA was verified using polyacrylamide and agarose gel electrophoresis, respectively. Synthesized IONPs and specially those functionalized with silica, chitosan and Tris

presented comparable desorption percentages with some reported studies in plasmid DNA separation. Remarkably, by using such functionalized IONPs, the DNA desorption times were more than ten-time faster than other similar reported adsorbents. Therefore, they can be considered for DNA extraction and purification from complex biological samples.

Keywords: Plasmid DNA isolation, functionalized iron oxide nanoparticles, coprecipitation.

Abbreviations: IONPs: Iron Oxide Nanoparticles, APTES: (3-aminopropyl)triethoxysilane, ODN: oligodeoxynucleotides, pDNA: Plasmid Deoxyribonucleic acid, Tris: tris(hydroxymethyl)aminomethane.

1. Introduction

Nanobiotechnology has become in a very promising field due to its several applications related to nanoscale systems [1, 2]. As an interdisciplinary science, it combines nanochemistry together with physics and molecular biology to develop novel functional materials. During the past decades, magnetic Iron Oxide Nanoparticles (IONPs) have been intensively studied not only for their fundamental technological applications but also for their unique advantages over other materials. For instance, magnetic IONPs are inexpensive to produce, biocompatible and environment-friendly [3]. Other properties such as chemical stabilization and functional surface determine various applications including Magnetic Resonance Imaging (MRI) [4], targeted drug delivery [5], hyperthermia, thermoablation treatment [6], bioseparation and biosensing [7, 8].

Among all these applications, magnetic separation has received considerable attention in biomedical research because functional magnetic particles can easily interact with selected biological targets. Magnetic separation of nucleic acids has several advantages compared to other traditional techniques such as column chromatography or extraction with toxic organic solvents [9]. The magnetic separation method provides the possibility of a direct isolation from crude samples, and therefore serves as a basis of various automated low- to high-throughput procedures that allow saving time and resources [10, 11]. Although various types of IONPs based kits for DNA isolation are commercially available [9], different functionalized IONPs can offer new possibilities for improving separation efficiency.

A key aspect to take into account in designing functionalized nanoparticles as solid phase support for DNA isolation is the nature of the interaction between biomolecules and nanoparticles surface [12]. By contrast with covalent immobilization, an electrostatic interaction is a suitable option in terms of automation and easy manipulation via pH switching. In this regard, several materials have been used to provide a charged surface for IONPs depending on pH media [13]. Polycations such as chitosan and other natural polysaccharides have been intensively described in the literature as coating materials for magnetic nanoparticles (MNP) [14]. Such polymers do not only provide a positively charge nanoparticle surface, but also they are readily available, inexpensive and biocompatible. For example, at pH below 6.4 chitosan polymer is cationic and can readily bind the anionic DNA molecules under these conditions [15].

On the other hand, silica and aminosilane compounds are very common in functionalizing nanoparticles (NPs) for DNA extraction and purification [16]. Other complex structures have been also reported; for instance, Tiwari *et al* have described the use of double-shell silica-chitosan IONPs for genomic DNA separation using pH response [17]. In this study, the composite showed all the potentialities of polymer based nanoparticles together with the advantages of silica compounds (biocompatibility and high nucleic acids affinity [11]). Similarly, Wu *et al* have reported the use of silica coated MNPs for plasmid DNA extraction. The methodology followed was very simple and it achieved a rapid isolation of plasmid DNA from crude cell lysates [18].

Tris(hydroxymethyl)aminomethane (Tris or Tromethamine) is considered a really available and functional compound in biotechnology. It is frequently used in different buffer solution preparations as well as a versatile pharmaceutical excipient. Recent reports have pointed out this compound as a high affinity ligand during the chromatographic purification or adsorption of lysozyme and bovine serum albumin [19, 20]. Tris-modified silica and magnetic microspheres have been also studied because of their hydrophilic interaction properties and protein purification potentialities. In this case, the elution behavior of proteins, nucleic bases and nucleotides was dependent on both media polarity and electrostatic interactions [21, 22].

Although Tris functionalized materials have been applied for protein purification and lysozyme separation, the isolation of nucleic acids by IONPs modified with Tris has not yet been fully explored. This research presents the synthesis and characterization of functionalized IONPs for plasmid DNA isolation. In addition, the system was compared with other well-established solid phase supports for DNA separation.

2. Materials and methods

2.1 Materials

Iron(II) sulphate heptahydrate ($FeSO_4{\cdot}7H_2O$), EDTA and aqueous ammonia (30%) were purchased from *Merck* Firm (Darmstadt, Germany). Iron(III) sulphate pentahydrate ($Fe_2(SO_4)_3.5H_2O$) and (3-aminopropyl)triethoxysilane (APTES) were supplied from *Fluka AG, Chem*. Glycerol, methanol and ethanol were obtained from *Panreac*. Low molecular weight chitosan, and sodium silicate (Na_2SiO_3) were purchased from *Sigma Aldrich*. In addition, PEG 6000 and Tris reagents were supplied from *Applichem Biochemica* and *GPR Rectapur*, respectively. The oligodeoxynucleotides used in preliminary isolation tests were synthesized in the Center for Genetic Engineering and Biotechnology, Havana, Cuba. (5´-TCTT CCCA GACG TGGA TTTC-3´). Plasmid DNA (pDisplay, 5.3 kb) was supplied from *Thermofisher*. All the chemicals were analytical grade and used without further purification. Deionized water was used throughout all synthetic experiments, while sterilized water was employed during nucleic acids isolation experiments.

2.2. Synthesis of iron oxide nanoparticles

Iron oxide nanoparticles were prepared by a modification of Massart's coprecipitation technique [23] using a rapid injection method. Typically, 0.682 g of $FeSO_4{\cdot}7H_2O$ and 1.225 g $Fe_2(SO_4)_3{\cdot}5H_2O$ were dissolved in 25 ml of deionized water and placed in a three-neck round bottom flask under nitrogen (N_2) atmosphere and continuous mechanic stirring at 60°C. Subsequently, 25 ml of aqueous ammonia solution was added abruptly in a rapid injection process to increase the pH value. After a black precipitate was formed, it was washed several times until the supernatant reached a pH value of 6.5. The precipitate was dried in a vacuum oven at room temperature for 24 h.

2.3. Post-synthesis surface functionalization

In order to evaluate DNA separation, four functionalized IONPs were synthesized. Two of them were accomplished using a post-synthesis surface modification (Figure 1).

a-) Silica coated IONPs (IONPs@SiO_2) were prepared following the sonochemical methodology of Chapa *et al* [24]. In a typical procedure, 1.30 ml of sodium silicate (Na_2SiO_3) was added in a flask together with 100 ml of deionized water and 0.200 g of previously synthesized iron oxide nanoparticles. After this, the mixture was sonicated for 30 minutes. As soon as the temperature of the mixture was increased to 80°C; hydrochloric acid (0.1 M) was added dropwise until a pH value of 6. The black precipitate was washed several times with deionized water by magnetic decantation. This coating procedure was repeated twice in order to ensure a silica coated IONPs surface.

b-) IONPs with an APTES shell (IONPs@APTES) provide a surface with free amino groups, which are very convenient for further synthetic steps or binding different biological molecules. The surface modification process was performed by dispersing 0.200 g of iron oxide nanoparticles in 900 µl of deionized water in a flask. Subsequently, 500 µl of glycerol and 100 µl of (3-aminopropyl)triethoxysilane (APTES) were added to the nanoparticle suspension under nitrogen atmosphere and vigorous stirring. Then, the system was heated at 90°C for 2 h. After cooling to room temperature, modified IONPs were recovered by using a permanent magnet and sequentially washed with deionized water and methanol. The solid was dried under vacuum at room temperature for 24 h.

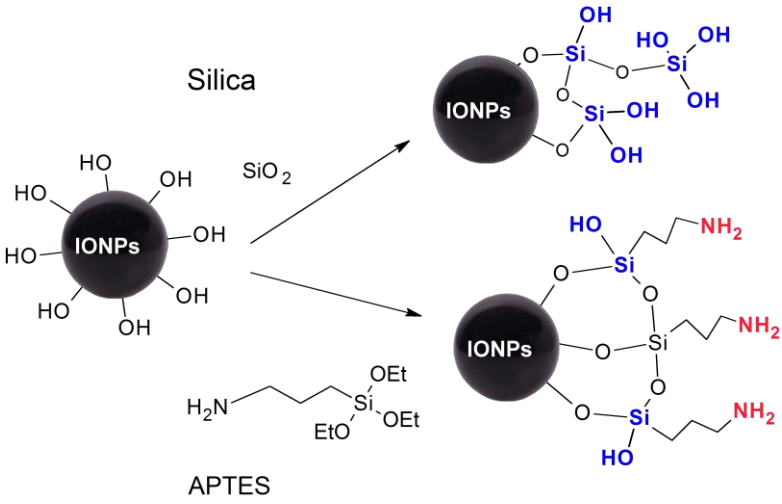

Fig. 1. Synthetic scheme for the preparation of silica and APTES functionalized IONPs.

2.4. In-situ surface functionalization

This approach consists on the co-precipitation of the iron oxides from a solution containing Fe(II), Fe(III), and the functional stabilizing agent. Two different nanoparticles were synthesized (Figure 2):

c-) Chitosan functionalized IONPs (IONPs@CHIT) were prepared as follows: A mixture of 2.779 g of $FeSO_4{\cdot}7H_2O$ and 3.919 g de $Fe_2(SO_4)_3{\cdot}5H_2O$ was placed in a three-neck round bottom flask under nitrogen atmosphere and continuous magnetic stirring at 50°C. Then, 0.125 g of chitosan in 5 ml of HCl (0.1 M) was added. Once Fe(II), Fe(III) and chitosan solution reached the desired temperature, and after 30 minutes, 20 ml of the aqueous ammonia solution was injected. The reaction was allowed to proceed for another 20 minutes. At the end of the reaction, the black precipitate was washed with deionized water and ethanol by magnetic decantation, and it was dried in a vacuum oven to obtain the final product.

d-) The preparation of magnetite nanoparticles coated with tris(hydroxymethyl)aminomethane (IONPs@TRIS) was carried out following a very similar methodology as above. Typically, 0.700 g of $FeSO_4{\cdot}7H_2O$ and 1.200 g of $Fe_2(SO_4)_3{\cdot}5H_2O$ were added to 25 ml of deionized water. This mixture was placed in a flask under continuous stirring and N_2 atmosphere. Successively, 0.200 g of Tris was added and the reaction was allowed to proceed for half an hour. After this, 25 ml of aqueous ammonia solution was abruptly injected. Once the dark brown precipitate was formed, it was washed several times with deionized water until a pH value of 6. Then, it was dried under vacuum for 24 h.

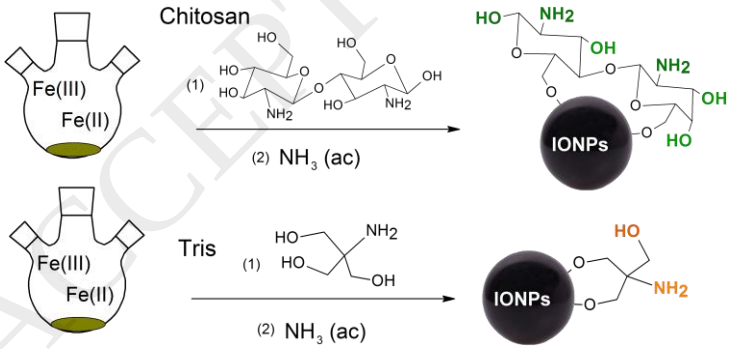

Fig. 2. Scheme of the *in-situ* surface functionalization of IONPs.

2.5. Determination of reactive amino groups on the nanoparticle surfaces

Dry aminofunctionalized nanoparticles (50 mg) were suspended in N,N-Dimethylformamide (DMF) by vortex and successively washed using magnetic decantation. At the same time, a mixture of 0.472 g Fmoc-Gly-OH and 0.216 g of Oxyma pure was prepared in DMF following a modification of the general procedure reported by Eissler *et al.* [25]. After total dissolution, 0.272 ml of N,N'-diiso-propycarbodiimide (DIC) were added to the mixture and then, quantitatively transferred to nanoparticles

(Coupling process). At that moment, the reaction was allowed to proceed for 1h under continuous agitation. For a second time, the system was magnetically decanted and sequentially washed three times with DMF, methanol and ether. The reaction completion was monitored using the Kaiser test [26]. Once the NPs were washed, they were dried under vacuum for 24 h.

In order to perform spectrophotometric measurements of nanoparticle amino groups loading, a certain amount of previously treated NPs was selected. After the addition of 500 µl piperidine solution 20%, the system was allowed to proceed for 30 min under continuous agitation. Finally, the supernatant containing the released Fmoc-piperidine adduct was transferred to a fresh tube and analyzed at 301 nm. This methodology was employed only for APTES, Chitosan and Tris functionalized IONPs in order to determine moles of reactive amino groups on nanoparticle surfaces per nanoparticle milligrams.

2.6. ODN and pDNA isolation using IONPs as solid phase support

ODN and pDNA isolation tests were accomplished using all IONPs (i.e. both unmodified and modified IONPs **a. b. c. d**.) In a typical adsorption procedure [1], 10 µl of IONPs dispersion was added to a fresh tube followed by the addition of 75 µl of binding buffer (1.25 M sodium chloride and 10% PEG 6000. pH=4). The IONPs dispersion was prepared from 1 mg dried IONPs in 500 µl of TE Buffer (10 mM Tris-HCl, 1 mM EDTA, pH=8). The suspension containing IONPs with the binding buffer was mixed in vortex together with 8 µl of ODN solution (0.25 µg/µl) and allowed to stand at room temperature for 3 min. The magnetic pellets were immobilized by an external magnet and the supernatant was removed. The pellets were washed with 70% ethanol and dried at room temperature. Immediately, 50 µl of TE buffer was added till resuspension and the system was incubated at 65°C with continuous agitation for 3 min. Then, magnetic nanoparticles were isolated again using magnetic separation. The supernatant containing desorbed ODN was transferred to another fresh tube and analyzed by means of spectrophotometric analysis at 260 nm and Polyacrylamide Gel Electrophoresis (PAGE) in denaturing conditions.

Plasmid DNA isolation tests were performed in the same conditions as above. The general protocol was quite similar. Once pDNA was isolated, it was quantified by UV-vis at 260 nm and agarose gel electrophoresis. In order to evaluate IONPs quantity influence during ODN and pDNA isolation, four experiments were carried out. During the first one, an aliquot volume of 10 µl IONPs suspension was added as previously described. After that, different experiments using aliquot volumes of 15, 20 and 25 µl were performed without any other variation.

Polyacrylamide Gel Electrophoresis (PAGE). A 15% acrylamide/7 M urea gel was prepared in the presence of 75 µl of ammonium persulfate 10% (APS) and 7.5 µl N,N,N′,N′-Tetramethylethylenediamine (TEMED) until polymerization. The running buffer was TBE 1x (15 g Tris-HCl, 20 mg boric acid, 17 mg EDTA in 10 ml of sterilized water). Electrophoresis was carried out at 200V for 40 min in a vertical unit (10 x 10 cm) coupled with an electrophoresis power supply from *Pharmacia Fine Chemical*. ODN presence was confirmed using a methylene blue 0.02% staining solution.

Agarose gel electrophoresis. A 1 % agarose gel containing ethidium bromide was run in a horizontal gel electrophoresis unit and LambdaDNA/ Marker HindIII from *Promega* was used. The running buffer was TBE 1x. Electrophoresis was carried out at 75V for 70 min. pDNA signals were showed using an UV transilluminator at 254 nm.

2.7. Instrumentation and characterization

The information related with average size distribution and morphology of IONPs was provided by **Transmission Electron Microscopy** studies (TEM). Digital micrographs were obtained in a JEOL TEM model 101 (300kV). In this occasion, the NP samples redispersed in water (by sonication) were cast onto a copper grid and dried by evaporation at room temperature. Images for IONPs@APTES were obtained in a FEI Tecnai20 (200 kV). The crystalline phase characterized by **Powder X-ray diffraction** (Cu Kα radiation source: λ=1.5418Å) was carried out in an X'pert-Pro diffractometer from PANalytical. In order to identify functional groups **Fourier-transform Infrared Spectroscopy** (FTIR) studies were performed. All spectra were collected in a WQF-510 spectrometer from Rayleigh firm. Magnetic measurements were

determined by means of a Physical Properties Measurement System (PPMS) from Evercool P525 Quantum Design in **Vibrating Sample Magnetometry** mode employing a 30 kOe magnetic field at 300 K. **Thermogravimetric Analysis** (TGA) was performed in a TGA Q5000 equipment using aluminum oxide as reference. Oligodeoxynucleotides and pDNA dissolution concentration was determined using an Ultrospec 2000 spectrophotometer from Pharmacia Biotech Firm. The same spectrophotometer was employed to measure the absorbance of the Fmoc-Piperidine adduct dissolution in order to determine reactive amino groups.

2.8. Statistical analysis

All data concerning to ODN or pDNA desorption percentages were found to be normally distributed. In addition, a multiple sample comparison was performed with a Fisher's Least Significant Difference (LSD) test to determine which means are significantly different from which others. Statistical significance was assumed when $p \leq 0.05$. The data related with particle size was expressed as mean$\pm$S.E.M (standard error of the mean) as a result of a log-normal fitting of the size histograms.

3. Results and discussion

3.1. Synthesis and surface modification

Uncoated IONPs were prepared by a coprecipitation process in aqueous media through the following reaction [6]:

$$Fe^{2+}{}_{(aq)} + 2Fe^{3+}{}_{(aq)} + 8OH^{-}{}_{(aq)} \rightarrow Fe_3O_{4\ (s)} + 4H_2O$$

This synthetic methodology is considered the easiest way to obtain IONPs like magnetite or maghemite. Also, it has shown to be a cost-effective and versatile technique for biomedical applications [27]. The main drawback of the coprecipitation method is the limited control on the particle size distribution, due kinetic factors involved during crystals growth. Moreover, nanoparticle surfaces are very reactive, so oxidation, or agglomeration processes take place [28]. In order to avoid such problems the surface of the nanoparticles was modified with silica, aminosilane, chitosan and Tris. The use of such capping agents provides stabilization of magnetic core and functional surface as well. The functionalization process was represented in figure 1 and 2. It resulted in obtaining magnetic nanoparticles with terminal amino, silanol or hydroxyl groups, which are very useful for further interaction with DNA molecules [13].

3.2. XRD characterization

The crystalline phase of every synthesized nanoparticle was characterized by X-Ray diffraction. Figure 3 shows the XRD patterns of each sample together with the standard powder diffraction pattern corresponding to the inverse spinel cubic structure of Fe_3O_4 NPs. In all cases a series of characteristic peaks (at 2θ = 30.16º, 35.50º, 43.03º, 56.96º, and 62.71º) were observed. These peaks were consistent with the standard pattern [3, 29]. This result indicates that surface modification did not change the crystal structure of IONPs. Furthermore, during magnetite NPs synthesis, some maghemite (γFe_2O_3) is often formed, showing a very similar XRD pattern. Thus, it is very difficult to guarantee only the presence of magnetite without some oxidized phase maghemite. Therefore, in these particular conditions XRD studies did not ensure the presence of maghemite characteristic reflections generally observed at low angle region [30]. In the case of the first four systems, sharp peaks indicate the highly crystalline nature of the nanoparticles. In contrast, the broad peaks observed for IONPs@TRIS pattern may correspond with small particle sizes or a low crystallinity degree [31].

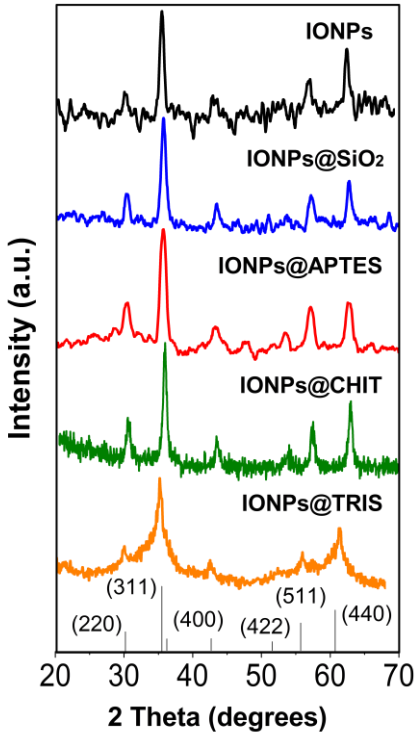

Fig. 3. XRD patterns of synthesized nanoparticles and the standard magnetite pattern [JCPDS #19-0629 (Fe_3O_4)].

3.3. Morphology and particle size analysis

In order to characterize particle size and morphology, transmission electron microscopy studies were performed. Figure 4 shows transmission electron micrographs and size distribution for both uncoated and silica-coated IONPs. In both cases, a quasi-spherical morphology was observed. Therefore, it is possible that after surface modification the particles maintained their original shape. In addition, a significant agglomeration was detected for uncoated IONPs, which can be attributed to the aggregation of individual particles because of unbalanced inter-particle forces or greater reactivity of nanoparticle surfaces [6, 32]. Particle size distribution was determined by statistical analysis using a log-normal distribution fitting. This analysis yielded an average particle size of 9.1 ± 0.1 and 9.8 ± 0.3 nm for IONPs and IONPs@SiO_2, respectively.

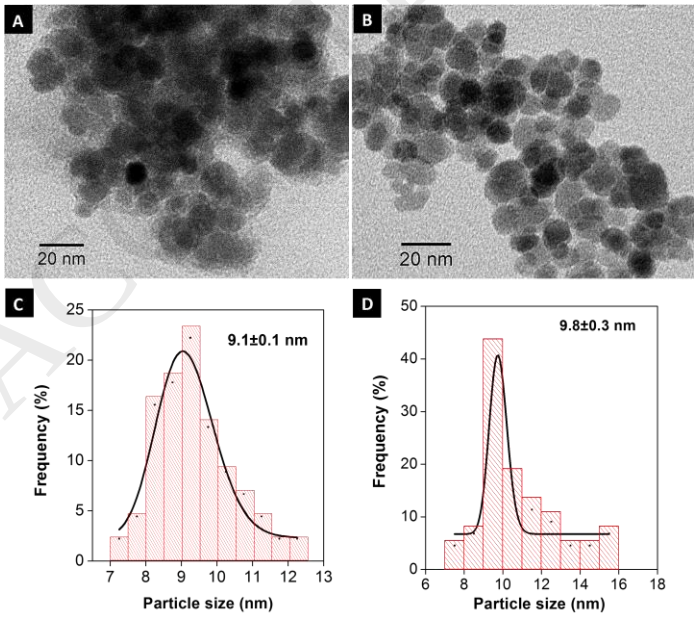

Fig.4. TEM images of uncoated (A) and silica-coated IONPs (B). Corresponding particle size distribution histograms (C, D).

APTES functionalized NPs micrograph (Figure 5, A) shows a nearly spherical morphology and slight aggregation. Average particle size was 12.1 ± 0.3 nm. In this sample, a uniform thin layer was observed (E) associated with a few nanometers APTES coating. In addition, measurements of a selected area of the transmission electron micrograph (B-C) showed characteristic lattice plane spacings. These measurements were approximately 2.56 and 1.60 Å, which are close to the expected spacings for the (311) and (511) planes of an inverse spinel structure of magnetite [33]. All this information is in accordance to the results obtained by X-Ray diffraction analysis (Supporting Information S1).

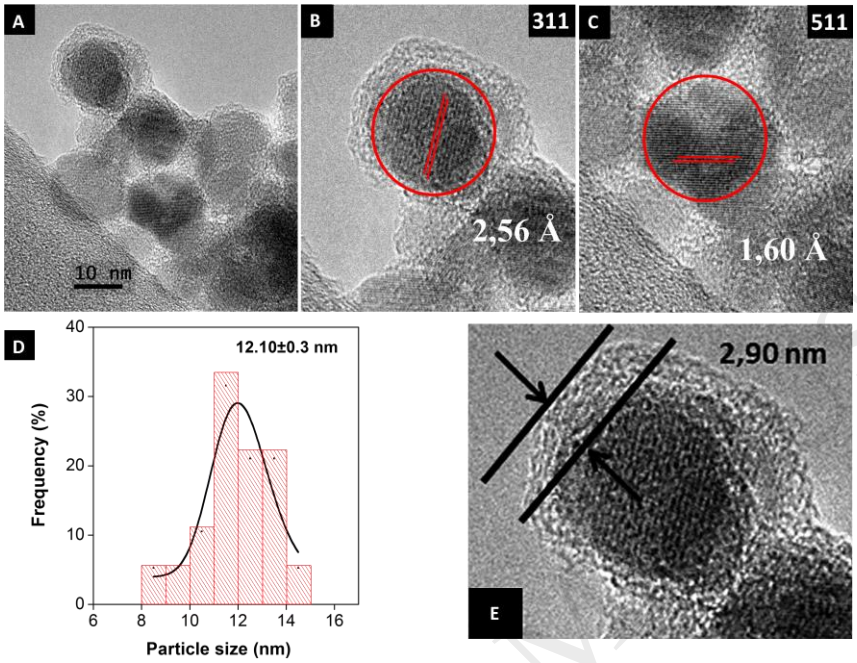

Fig. 5. TEM image of APTES-coated IONPs (A) and the selected area of the micrograph for plane-spacings measurements (B-C). Size distribution (D) and thin layer APTES coating of IONPs (E).

TEM micrographs of chitosan and Tris modified IONPs appear in figure 6 (A and B, respectively). The *in-situ* synthesis of functionalized IONPs with chitosan yielded an average size of 12.1 ± 0.4 nm. Also, a quasi-spherical morphology was observed. In the individual case of IONPs@TRIS, very small NPs with average sizes of 2.6 ± 0.1 nm were obtained. This result agrees with XRD observations and may be associated with a stabilizer agent excess. Furthermore, temperature during the synthetic process could play an important role in terms of crystallinity; therefore, it is possible that some amorphous NPs were formed [31].

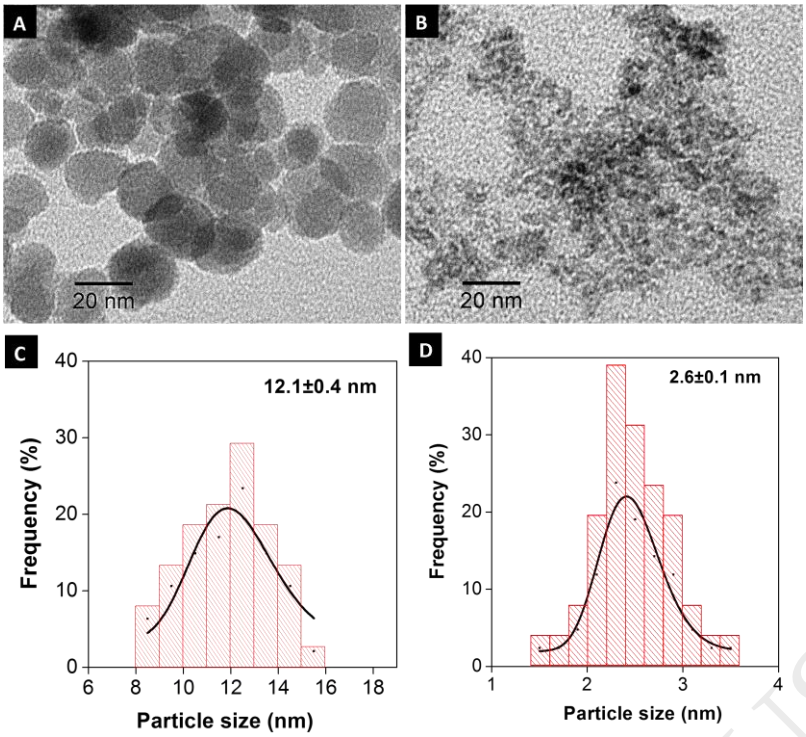

Fig. 6. TEM images of chitosan (A) and Tris-coated IONPs (B) and their size distributions (C-D).

3.4. FT-IR characterization

In order to confirm the functionalization of IONPs surface, FTIR analysis was used. Figure 7(A) shows the FTIR spectra of IONPs together with those nanoparticles functionalized in a second step. In all cases, a characteristic absorption band was observed in the range of 547-590 cm^{-1} mainly associated with Fe-O vibrations in iron oxide nanoparticles [33, 34]. Another broad band at about 3300 cm^{-1} and a weak one at 1634 cm^{-1} were observed corresponding to O-H stretch and δ_{H-O-H}, respectively. This fact is attributed to the presence of adsorbed water in the nanoparticle surface [35]. Silica network is often adsorbed on the magnetite surface through Fe-O-Si bonds. The signals associated with this particular vibration cannot be seen in the IR spectra because it appears at around 584 cm^{-1} and therefore overlaps with Fe-O vibrations. [36]. So, the adsorption of silane polymer as well as silica onto the surface of IONPs was confirmed by bands at 1066 and 960,800 cm^{-1} assigned to the SiO-H and asymmetric-symmetric vibrations of Si-O-Si groups, respectively. The two broad bands at around 3450 and 1622 cm^{-1} can be attributed to N-H stretching vibration and NH_2 bending mode of free amino group, respectively. Furthermore, hydrogen-bonded silanols also absorb at 3200 cm^{-1} approximately. The presence of anchored propyl groups was confirmed by a weak signal associated with C-H stretching vibrations at about 2931 cm^{-1} [37-39]. In the case of IONPs@APTES spectrum, the existence of a double band in the place of Fe-O vibrations can be ascribed to some oxidation or maghemite formation [33].

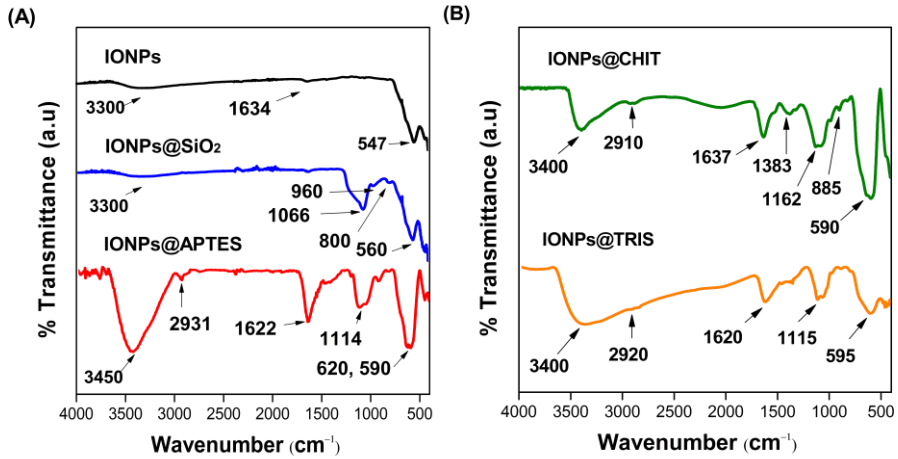

Fig. 7. FTIR spectra of synthesized NPs. Second-step functionalized IONPs (A) and *in-situ* modified IONPs (B).

The success of chitosan and Tris grafting onto the IONPs was also qualitatively verified. FTIR spectra of such functionalized nanoparticles were presented in figure 7(B). The chitosan coated IONPs spectrum showed their characteristic absorption band in the range of 3650-3000 cm^{-1} that correspond with OH groups stretching vibrations, which are overlapped with N-H stretching vibrations from free amino groups. Also, C-H vibrations appear in the spectrum as a very weak band at around 2910 cm^{-1}. The characteristic absorption bands at 1637 and 1383 cm^{-1} are associated with amine and methylene bending vibrations, respectively [40]. Absorption in the range of 1160-1000 cm^{-1} has been attributed to CO group with the distinctive peak at 1162 cm^{-1} of C–O–C stretching vibration for ether groups and skeletal vibration of the glucosamine residue [41]. Moreover, the small peak at around 885 cm^{-1} can be ascribed to wagging of the saccharide structure of chitosan [42] and the characteristic absorption band at 590 cm^{-1} to Fe-O vibration of IONPs.

Tris-modified IONPs spectrum shows five characteristic absorption bands associated with its structure. In general, Tris molecule presents three OH groups per molecule together with an amino group. Thus, the main vibrations appear at 3400 cm^{-1} (O-H and N-H stretching vibrations), 2920 (C-H stretching vibrations) and 1620 (N-H bending vibrations). The broad peak at around 1115 cm^{-1} can be attributed to CO vibrations and the absorption band at 595 cm^{-1} is characteristic of Fe-O vibration from iron oxide structure.

3.5. Thermogravimetric analysis

The results of TGA characterization of unmodified IONPs and those functionalized are shown in figure S2 of the Supporting Information. From these measurements, an initial mass loss until 200 ºC is generally verified. This is due to surface dehydration of IONPs, i.e. desorption of physically and chemically adsorbed water, respectively (typical of a coprecipitation process in aqueous media) [35]. It is noticeable in all samples, a weak mass loss in the range of 500-650 ºC. This fact is attributed to characteristic phase transitions in iron oxide nanoparticles. This is, magnetite NPs oxidized to maghemite and finally to hematite, which is the more thermodynamically stable phase of IONPs. This process was barely detected for IONPs@APTES and it is influenced for particle size. For instance, larger size NPs, such as uncoated IONPs and those modified with silica and chitosan exhibit a phase transition temperature of 620, 624 y 630 ºC, respectively. By contrast, IONPs@TRIS have a phase transition temperature of 552 ºC. Consequently, smaller size NPs exhibit a lower phase-transition temperature. According to a study developed by Chen Y.H., this behavior could be attributed to the excess energy stored on the surface of smaller particles [43]. Thus, it suggests that Tris functionalized IONPs present higher surface energy, and hence, a lower temperature (or less energy) is required to produce phase transitions.

TGA measurements also allowed to confirm the presence of the coating material in all samples. For instance, uncoated IONPs showed a mass loss until 300 ºC approximately. The weight loss occurred in

two different stages. The first one between 98 – 100 °C corresponds to adsorbed water. The second stage observed was between 190-270 °C and it is mainly attributed to a degradation of hydroxyl groups, respectively [44]. For silica and APTES modified IONPs, an average mass loss of 4 and 6% was calculated (Table S2 in Supporting Information). These values represented a mass loss due to organic material degradation in the range of 200-450 °C. Also, chitosan functionalized-IONPs presented an average mass loss of 8% related with organic material degradation. In the precise example of Tris-modified IONPs, stabilizer material degradation was slightly different from previous systems. An average mass loss of 13% was calculated. This fact can be associated with some coating material excess.

3.6. Magnetic properties

The magnetic behavior of all samples was analyzed by Vibrating Sample Magnetometry. Figure 8 shows the magnetization curves of both uncoated and functionalized IONPs. From these results it can be observed, that saturated hysteresis loops formation confirms the magnetic nature of IONPs [45]. Table 1 contains information about the main parameters of M-H curves. It is noticeable that all samples showed high saturation magnetization (Ms) values, except for those NPs functionalized with Tris.

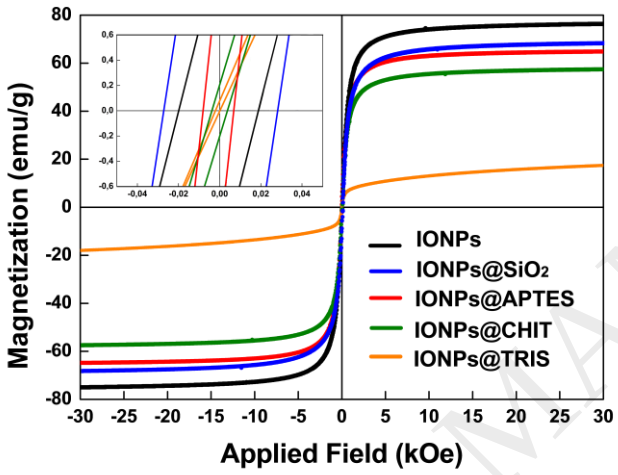

Fig. 8. Magnetic hysteresis loops of unmodified and modified IONPs.

The main difference between Ms values of the IONPs and the bulk material (82-92 emu/g) [33, 46] can be explained in terms of the nanometric sizes and then noticeable surface effects. The surface of the nanoparticles is considered to be composed of some canted or disordered spins that prevent the core spins from aligning along the field direction, resulting in a decrease of the saturation magnetization of the small size particles. This phenomenon is referred to as 'spin canting' [47, 48]. In addition, high crystallinity results in higher saturation magnetization. Another important feature in the set of samples is the lower values of residual magnetization (Mr) and the intrinsic coercivity (iHc). This singularity is characteristic of a nearly superparamagnetic behavior [49].

Table 1. Particle size and magnetic parameters of all synthesized NPs.

NPs	Particle size (nm)	Ms (emu/g)	Mr (emu/g)	iHc (Oe)
IONPs	9.1±0.1	75.72	1.33	20.11
IONPs@SiO_2	9.8±0.3	68.23	3.09	28.41
IONPs@APTES	12.1±0.3	64.80	1.50	20.24
IONPs@CHIT	12.1±0.4	57.45	0.15	3.32
IONPs@TRIS	2.6±0.1	17.60	0.06	2.41

A decrease of saturation magnetization was observed for the post-synthesis functionalized IONPs mainly associated with the coating material. For instance, IONPs have a saturation magnetization value of 75.72 emu/g; this value decreases by 10% with silica modification, and 15% with an APTES shell presence.

Saturation magnetization is a property that indicates the statistical average of the magnetic moments in the direction of the external magnetic field. In this situation, there are two materials, but only IONPs core has a magnetic response and this property is divided by the total mass of the system (i.e. IONPs + coating material) [24]. Thus, it is expected that modified IONPs present lower Ms values in comparison with uncoated IONPs.

In the case of the *in situ* functionalized IONPs, it was observed that high saturation magnetization values were obtained for chitosan-coated nanoparticles. By contrast, Tris functionalized MNPs showed a low saturation magnetization value. This fact can be attributed with small size NPs formation in agreement with TEM and XRD observations [31]. According to Qing Li *et al*., many factors such as particle size, shape, domain structure and crystalline order direct influence magnetic properties [50]. In this regard, small size IONPs, affect their magnetic properties especially the intrinsic coercivity and saturation magnetization [51]. Those parameters are fundamental during magnetic manipulation studies such as bioseparation. However, in this research the low Ms value for IONPs@TRIS, was not a problem because three minutes for magnetic separation assays using the synthesized systems were more than enough to successfully separate a high percentage of ODN or pDNA amount.

3.7. Determination of free amino groups on nanoparticle surfaces

For most of the functionalized nanomaterials, the amino groups modification process is fundamental in many biomedical applications. Normally, it is the first active group to be introduced [52]. In DNA isolation, reactive amino groups on nanoparticle surfaces, play an important role during the adsorption stage. It has been reported that such amino groups are responsible for the electrostatic interactions with the negatively charged DNA molecules [15]. Assays of amino group-containing compounds, for instance amino acids, peptides, and polymers, generally employ a colorimetric assay, such as 2,4,6-trinitrobenzenesulfonic acid (TNBS) [53] or Kaiser test [26]. However, a fluorescent or spectrophotometric determination of dibenzofulvene–piperidine adduct has gained a lot of attention in the last decades [54]. Compared with elemental analysis, or acid-base titrations for amino groups quantification, spectrophotometric assays can determine the amount of active groups rather than a total amount.

In solid-phase peptide synthesis (SPPS), the Fmoc-derived groups have evolved as the dominating protecting groups for temporary amine protection. This base-labile group is quantitatively cleaved with 20% (v/v) piperidine in DMF, forming the dibenzofulvene–piperidine adduct (Fig 9). This adduct exhibits two distinct UV absorbance maxima at $\lambda = 301.0$ and 289.8 nm. Absorption values measured at either of the absorbance maxima can be used, in combination with the respective molar absorption coefficient, to calculate the substitution of Fmoc-protected structures. Considering all those features, this procedure has become in a very robust analytical test method for amino groups quantification [25].

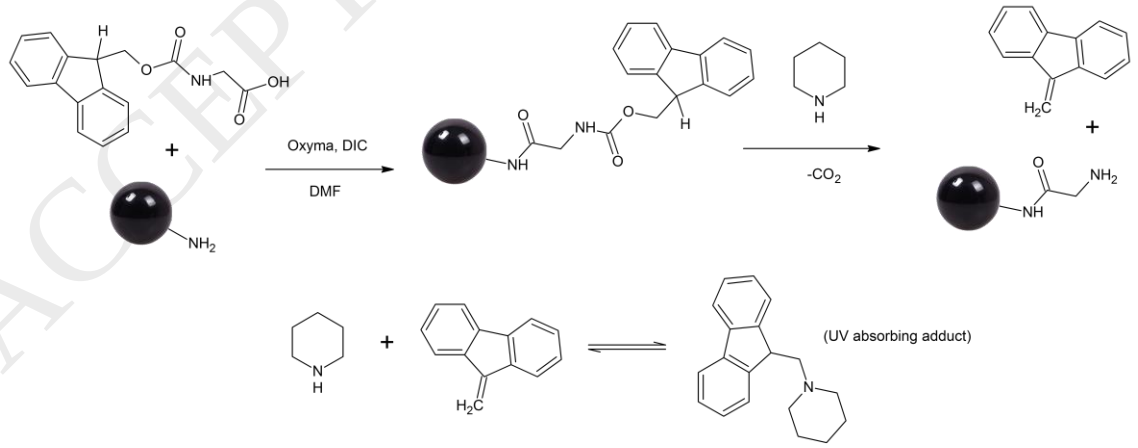

Fig. 9. Fmoc-Gly-OH cleavage with 20% (v/v) piperidine and formation of the dibenzofulvene–piperidine adduct.

In the studied case, three aminofunctionalized IONPs were employed. The source of amino groups in such nanomaterials was the APTES and Tris molecules as well as the chitosan polymer. These coating

agents were qualitatively characterized by means of infrared spectroscopy and thermogravimetric analysis. One of the main advantages of these IONPs are their magnetic properties, which are very convenient during the cleavage methodology. In this regard, table 2 presents the amount of substance related with amino groups per nanoparticle milligrams. These results were derived from the spectrophotometric analysis of the dibenzofulvene–piperidine adduct, which is proportional to the amount of reactive amino groups on the nanoparticle surfaces.

Table 2. Free amino groups quantification on the nanoparticle surfaces

NPs	nmoles of amino groups/NPs milligrams
IONPs@APTES	47.13 nmol/mg
IONPs@CHIT	24.35 nmol/mg
IONPs@TRIS	121.28 nmol/mg

As reported in table 2, APTES functionalized NPs revealed a low amount of exposed amino groups in comparison with IONPs@TRIS. This fact can be attributed with the complexity of the nanoparticle surface. Van de Waterbeemd *et al.* have hypothesized that a 'multilayer' of condensed silane structures form on the surfaces of the materials, where most of the amine groups can be sequestered as 'internal' groups and therefore undetectable using spectrophotometric assays [55]. All the amino silane activated materials possess ratios of surface to sequestered/internal amino groups between 1:2 and 1:3. In the case of chitosan, the low value could be influenced by the type of interaction between chitosan and the iron oxide nanoparticle surface. For instance, Dyawanapelly *et al*. have explored the electrostatic binding between positively charged chitosan and the nanoparticle surface. This is, the amino groups are responsible for the surface attachment and then, the hydroxyl groups remain exposed as a result of the modification process [56]. This fact can interfere the amino quantification due to compromised groups. In the particular case of Tris modified IONPs, a value of 121.28 nmol/mg was obtained. This means a higher amount of amino groups on the nanoparticle surface. As referred before and considering the TEM analysis, very small nanoparticles were synthesized. Then, a large surface area involves many active sites for Tris molecules attachment and therefore available amino groups.

3.8. Preliminary ODN and pDNA separation assays

Separation assays were performed in order to compare all synthesized NPs as solid phase support in ODN and pDNA isolation. According to Ghaemi *et al.*, DNA adsorption is a very complex process. It depends on many factors such as DNA concentration, temperature, contact time, pH media, etc. All these experimental constraints should be carefully optimized [12]. Nevertheless, in this research only nanoparticle amount was varied keeping the other parameters as a constant.

Throughout the first stage of the separation assay, synthetic ODN were employed. They represent a useful model to study nucleic acids interaction with functional surfaces and can confirm biomolecule immobilization. ODN were used in the first place as a starting reference in magnetic separation of pDNA. Isolation protocol involves surface charge modulation using pH control. According to Ming *et al*., the mechanism for DNA interaction with functionalized IONPs is similar to carboxyl-terminated magnetic particle purification systems, in which the double stranded DNA is thermodynamically adsorbed on the particle surface in the presence of a polyethylene glycol and sodium chloride [57]. In that case, binding buffer interact with both unmodified and functionalized IONPs providing a positive charged surface, this is, at a pH value of 4, hydroxyl and amino groups are protonated ($-OH_2^+$, $-NH_3^+$). Under these conditions and taking advantage of electrostatic interactions, magnetic nanoparticles easily interact with negatively charged phosphate backbone from ODN or DNA molecules [13]. Additionally, the presence of protonated groups develops favorable hydrogen bonding interactions [12]. Once DNA molecules are immobilized on NPs surface they can be released by increasing pH. In this situation, elution or TE buffer, eventually causes a sharp diminish of protonated groups. Figure 10 shows separated ODN and pDNA mass using all nanoparticles as a solid phase support. In these graphs the concentration or mass, were estimated from absorbance spectrophotometric measurements at 260 nm. It is important to notice that ODN/pDNA mass was plotted versus the amount of synthesized NPs in the selected aliquot volume.

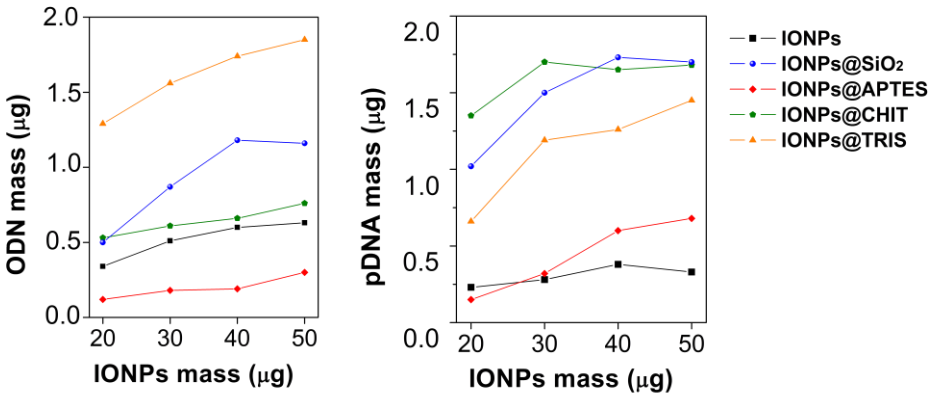

Fig. 10. Separated ODN/pDNA amount using the magnetic NPs as a solid phase support.

It can be observed that biomolecule separation by most of the functionalized IONPs is higher than that when using unmodified IONPs. In both graphs, uncoated NPs and those modified with APTES showed lower separation values. As reported in literature, unmodified IONPs have a tendency to aggregate into large clusters and thus lose important properties associated to nanometric scale such as surface area. Furthermore, they are also sensitive to oxidation and this process is a key in magnetic properties [58]. The problem with APTES functionalized IONPs could be associated with the particular conditions used during this research (separation protocol) [59], as well as agglomeration according with TEM measurements showed in figure 5. It appears, moreover, that in this example, the elution time could be influencing the desorption process [60].

In the case of chitosan, silica and Tris modified IONPs the ODN/pDNA separated amount was higher than those separated with both uncoated and APTES modified IONPs. During pDNA separation, these particular NPs showed better results, even with 30 μg of modified IONPs. The use of Tris as coating material for the magnetic core together with the synthesis conditions, led the formation of small IONPs. This feature resulted in a high surface area and therefore more adsorption sites for oligos and DNA molecules. It is noticeable that biomolecular separation decreased in the case of pDNA separation with IONPs@TRIS compared with ODN separation. Among plasmid DNA conformations, supercoiled (or covalently closed circular (CCC) form) differs from the others in terms of the structure and biological role. For instance, Poly *et al.* reported a comparative adsorption study between linear and supercoiled pDNA on clay minerals. In this study, the main differences were associated with the density and availability of free phosphate groups [61]. It can be assumed that in CCC plasmid DNA, only phosphate groups concentrated at the maximum bending of supercoiled molecules would be available and involved in adsorption, whereas most of the phosphate moieties localized within the supercoiled molecule cannot influence adsorption. In contrast to plasmid DNA, ODN expose a higher number of available phosphate groups. These anionic charges should establish a higher contact (electrostatic interactions) with the positively charged nanoparticle surface. This different distribution and accessibility of charges on both biomolecules may explain the difference between adsorption behavior of supercoiled pDNA and ODN, respectively.

Desorption percentage is an important parameter to report in regeneration and reusability studies [12]. The desorption ratio was calculated taking into account the last point in the figure 10 graphs; this is, the ODN/pDNA separated amount with the maximum quantity of IONPs employed (50 μg). Equation 1 was used to calculate desorption percentage, where c_I is the separated ODN/pDNA concentration, c_0 is the initial biomolecule concentration and *D%* is the desorption percentage for all nanoparticle samples.

$$D\%. = \frac{c_i}{c_0} \times 100 \qquad (1)$$

Figure 11 shows a comparative chart plotting desorption percentage for every IONPs. It can be observed that the particles with higher pDNA desorption percentages were those functionalized with silica, chitosan and Tris. This aspect means that, during pDNA separation, the *D%* showed significant

differences for those NPs in comparison with APTES and uncoated NPs. In the individual case of Tris functionalized IONPs a *D%* of 93 was calculated for ODN separation. In fact, this was the highest *D%* obtained for the set of samples and was very high for pDNA separation as well (73%) (a detailed explanation concerning the statistical analysis procedure was reported in supporting information S3).

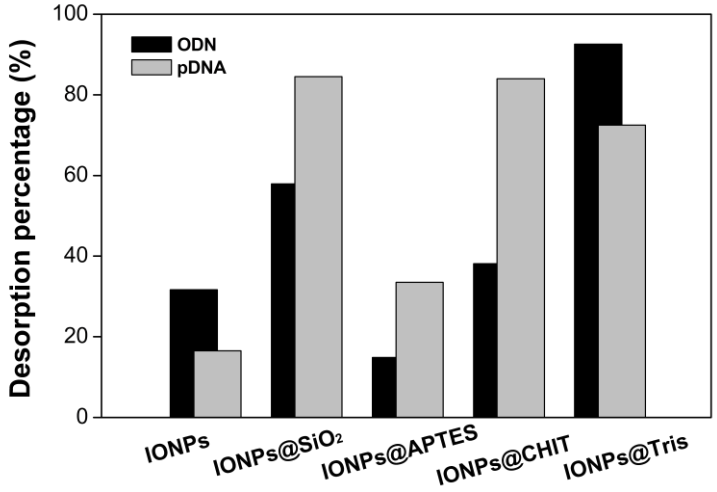

Fig. 11. Comparative chart with calculated *D%* for every system during ODN/pDNA separation.

As reported in the literature [16], silica modified magnetite nanoparticles significantly enhance the isolated DNA amount. This fact can be attributed with the high chemical stability, selectivity and nucleic acids affinity of the silica network [11]. Chitosan polymer as well as Gelatin and Polyethylenimine (PEI) have been successfully employed in DNA separation and amplification [15]. Such important polycations improves DNA separation efficiency due to the presence of protonated amino groups and their electrostatic interactions with DNA molecules. These functionalized particles recovered twice as much than the phenol-chloroform extraction technique [1]. In the present study, a new Tris functionalized IONPs was compared with coated and unmodified NPs for the separation of pDNA. The statistical analysis showed that Tris modified IONPs had the greatest significant differences related with pDNA *D*% in comparison with the other nanoparticles. For ODN *D*%, a similar situation was observed (Supporting information S3). This trend could be explained in terms of amino groups amount on the nanoparticle surface. As reported in section 3.7, Tris functionalized nanoparticles showed the highest amount of reactive amino groups, which means several groups available to interact with the negatively charged ODN or DNA molecules.

3.9. Evaluation of ODN/pDNA integrity by electrophoresis

The quality of the separated ODN was determined by polyacrylamide gel electrophoresis, which is a qualitative technique for ODN integrity studies. As showed in Supporting information (figure S3A), lanes 2-6 contain separated ODN with all nanoparticles and lane 1 has the ODN control (2 μg starting amount). In this case, a single band similar to control was detected without any smear. This means no apparent ODN degradation [59], so, at least separated ODN did not undergo fragmentation. Plasmid DNA integrity was also checked by agarose gel electrophoresis. In the figure S3B, lanes 3-7 contain separated pDNA with all nanoparticle samples. It can be observed a single band running at the same level of the pDNA control (lane 2) without degradation smears. These results suggested that adsorption process did not affect pDNA integrity, which is particularly useful for downstream applications. Also, from the agarose electrophoresis image it can be identified a wide band corresponding to a supercoiled pDNA conformation, which is characterized by tightly packed structure with limited spatial availability of nitrogen bases [61, 62].

Considering the above results, the synthesized magnetic nanoparticles were compared with other reported adsorbents. Table 3 shows a summary of main calculated parameters during the adsorption study. When

compared with other well-established adsorbents in general, the functionalized NPs synthesized in this research showed good results. For instance, an average desorption percentage of 80 % between silica, chitosan and Tris modified IONPs is comparable with APTES and silica modified NPs (A-MNPs and M-MSN, respectively) or graphene oxide (G. oxide). In terms of desorption time, synthesized NPs showed an extremely lower desorption time than those reported in table 3. This is a very important feature of the synthesized adsorbents in this research. Also, it represents a step forward in the synthesis and characterization of new potential Tris functionalized IONPs.

Table 3. Adsorption related information of functionalized IONPs in comparison with other reported adsorbents during DNA separation.

Adsorbents	**Method**	**Desorption time**	**D%**	**Ref.**
A-MNPs	Fluorescence	40 min	85	[63]
M-MSN	UV/vis	60 min	~90	[64]
Soil minerals	UV/vis	120 min	78	[65]
G. oxide	Fluorescence	720 min	~80	[66]
IONPs@TRIS	UV/vis	3 min	~73	This work
IONPs@CHIT	UV/vis	3min	~84	
IONPs@SiO_2	UV/vis	3min	~85	

4. Conclusions

The development of new synthetic materials to manipulate biological entities is to date a challenging problem in biotechnology. In this research, it was synthesized and characterized five different IONPs, with potential applications in DNA separation. Preliminary separation assays were performed with ODN and plasmid DNA, which showed high desorption percentages for silica, chitosan and Tris functionalized IONPs. By using such functionalized IONPs, the DNA desorption time was more than ten-time faster than other similar reported adsorbents. Furthermore, the methodology followed was very simple, quick, cheap and does not require the use of organic solvents. Separated pDNA showed a good integrity, which is useful for further activities, such as gene delivery, vaccines preparation, and diagnosis purposes.

Acknowledgements

The authors acknowledge Dr. Edilso Reguera from the Center for Applied Science and Advanced Technology of IPN, Legaria Unit, Mexico for the access to their experimental facilities. The authors also thank MSc. Greter A. Ortega (FQ-UH) and Dra. Linnavel Jiménez Hernández (IMRE-UH) for XRD and TGA measurements. Special acknowledgements to the peptide synthesis group from Center for Genetic Engineering and Biotechnology (CIGB).

Conflicts of interest: The authors declare no conflict of interest.

References

[1] Rahnama H, Sattarzadeh A, Kazemi F, Ahmadi N, Sanjarian F, Zand Z. Comparative study of three magnetic nano-particles (Fe_3O_4, Fe_3O_4/SiO_2, $Fe_3O_4/SiO_2/TiO_2$) in plasmid DNA extraction. *Analytical Biochemistry*. **2016;** 513 68-76.

[2] Grazú V, Moros M, Sánchez-Espinel C. "Chapter14-Nanocarriers as nanomedicines: design concepts and recent advances," in Frontiers of Nanoscience Nanobiotechnology Inorganic Nanoparticles vs Organic Nanoparticles, eds J.M. de la Fuente and V.Grazu (Oxford, UK: Elsevier). **2012**; 337–440.

[3] Wu W, Wu Z, Yu T, Jiang C, Kim WS. Recent progress on magnetic iron oxide nanoparticles: synthesis, surface functional strategies and biomedical applications. *Sci. Technol. Adv. Mater*. **2015**; 023501: 1-3.

[4] Veiseh O, Gunn J, Zhang. Design and fabrication of magnetic nanoparticles for targeted drug delivery and imaging. *Advanced Drug Delivery Reviews.* **2010**. 62: 284-304.

[5] Laurent S, Saei A-A, Behzadi S, Panahifar A, Mahmoudi M. Superparamagnetic iron oxide nanoparticles for delivery of therapeutic agents: opportunities and challenges. *Expert Opin. Drug Deliv*. **2014**; 14:2.

[6] Laurent S, Forge D, Port M, Roch A, Robic C, Vander Elst L, Muller R. Magnetic Iron Oxide Nanoparticles: Synthesis, Stabilization, Vectorization, Physicochemical Characterizations, and Biological Applications. *Chem. Rev*. **2008**; 108: 2066-2068.

[7] Zhang W, Li X, Zou R, Wu H, Shi H, Yu S, Liu Y. Multifunctional glucose biosensors from Fe_3O_4 nanoparticles modified chitosan/graphene nanocomposites. *Sci. Rep*. **2015**, 5:1.

[8] Min J, Woo M-K, Young H, Woo J, Hua J, Lim C-S, Keun Y. Isolation of DNA using magnetic nanoparticles coated with dimercaptosuccinic acid. *Anal. Biochem*. **2014**; 447: 114.

[9] Berensmeier S. Magnetic particles for the separation and purification of nucleic acids. *Appl. Microbiol. Biotechnol*. **2006**; 73:495–504.

[10] Köse K. Nucleotide incorporated magnetic microparticles for isolation of DNA. *Process Biochemistry*. **2016**. 1359-5113.

[11] Berensmeier S. Magnetic particles for the separation and purification of nucleic acids. *Appl Microbiol Biotechnol*. **2006**; 73:495–504.

[12] Ghaemi M, Absalan G. Study on the adsorption of DNA on Fe_3O_4 nanoparticles and on ionic liquid-modified Fe_3O_4 nanoparticles. *Microchim Acta*. **2014**; 181: 45-53.

[13] Pershina A, Sazonov A, Filimonov V. Magnetic nanoparticles-DNA interactions: design and applications of nanohybrid systems. *Russian Chemical Reviews*. **2014**. 83:299-322.

[14] Uthaman S, Lee S, Cherukula K, Cho C-S, Park I-K. Polysaccharide-Coated Magnetic Nanoparticles for Imaging and Gene Therapy. *BioMed Research International*. **2015**. 1-14.

[15] Pandit K, Nanayakkara I, Cao W, Raghavan S, White I. Capture and direct amplification of DNA on chitosan microparticles in a single PCR-Optimal solution. *Anal. Chem*. **2015**, 87:11022-11029.

[16] Kazerooni H, Abdolmalaki A, Nasernejad B, Chavoshi A. Novel biocompatible pegylated amino-silane modified superparamagnetic@silica core-multishell nanospheres in nuclear nano-biomedical. *Canadian Journal on Biomedical Engineering & Technology*. **2011**. 2: 1.

[17] Tiwari A, Satvekar R, Patil P, Karande V, Raut A, Rohiwal S, Shete P, Ghosh S, Pawar S. Magneto-separation of Genomic Desoxyribose Nucleic Acid using pH Responsive Fe_3O_4@silica@chitosan Nanoparticles in Biological Samples. *RSC Advances*. **2014**; 26:3.

[18] Biao W, Lian X, Lina C, Xian Z, Rong S. Isolation and purification of plasmid DNA by silica coated magnetic nanoparticles. *Chinese Journal of Biochemistry and molecular biology*. **2009**; 25:958-962.

[19] Zhang G, Cao Q, Li N, Li K, Liu F. Tris(hydroxymethyl)aminomethane-modified magnetic microspheres for rapid affinity purification of lysozyme. *Talanta*. **2011**; 83:1515-1520.

[20] Zhang B, Wang Y, Gao M, Gu M, Wang C. Tris(hydroxymethyl)aminomethane-functionalized agarose particles: parameters affecting the binding of bovine serum albumin. *J Sep Sci*. **2012**, 35(12):1406–1410.

[21] Bui, N. T. H., Verhage, J. J., Irgum, K. Tris(hydroxymethyl)aminomethane-functionalized silica particles and their application for hydrophilic interaction chromatography. *J. Sep. Sci.* **2010**, 33, 2965–2976.

[22] Quan, L., Cao, Q., Li, Z. Y., Li, N., Li, K. A., Liu, F. Highly efficient and low-cost purification of lysozyme: A novel tris(hydroxymethyl)aminomethane immobilized affinity column. *J. Chromatogr. B*. **2009**, 877, 594–598.

[23] Massart R. Preparation of Aqueous Magnetic Liquids in Alkaline and Acidic Media. *IEEE Transactions on Magnetics*. **1981**; 17:1247-1248

[24] Chapa C, Martinez C, Martinez A, Olivas I, Zavala O, Garcia P. Development of Antibody-Coated Magnetite Nanoparticles for Biomarker Immobilization. *Journal of Nanomaterials*. **2014**; 1.

[25] Eissler S, Kley M, Bächle D, Loidl G, Meier T, Samson D. Substitution determination of Fmoc-substituted resins at different wavelengths. *Journal of Peptide Science*. **2017**; 23:757-762.

[26] Kaiser, E., Colescot, R. L., Bossinge, C. D. & Cook, P. I. Color test for detection of free terminal amino groups in solid-phase synthesis of peptides. *Anal. Biochem*. **1970**; 34, 595-598.

[27] Figuerola A, Di Corato R, Manna L, Pellegrino T. From iron oxide nanoparticles towards advanced iron-based inorganic materials designed for biomedical applications. *Pharmacological Research*. **2010**; 62:127.

[28] Durdureanu-Angheluta A, Pinteala M, Simionescu B. Tailored and Functionalized Magnetite Particles for Biomedical and Industrial Applications. *Materials Science and Technology. InTech Publishing*. **2012**; 154.

[29] Hammond C. The Basics of Crystallography and Diffraction. Third Edition. Oxford science publications. **2009**: 36-37.

[30] Kim W, Yul C, Wook S, Min K, Kwon H, Song K, Jin I. A new method for the identification and quantification of magnetite-maghemite mixture using conventional X-ray diffraction technique. *Talanta*. **2012**; 94:348-352.
[31] Phu N, Ngo D, Hoang L, Luong N, Hai N. Crystallization process and magnetic properties of amorphous iron oxide nanoparticles. *Journal of Physics D Applied Physics*. **2011**; 1.
[32] Wu W, Zhong C, Roy V. Designed synthesis and surface engineering strategies of magnetic iron oxide nanoparticles for biomedical applications. *Nanoscal*e. **2016**; 8:19421.
[33] Rochelle M. Cornell, Udo Schwertmann-The Iron Oxides Structure, Properties, Reactions, Occurrences and Uses, Second Edition-Wiley-VCH Verlag GmbH & Co. KGaA, Weinheim. **2003,** 9, 119-130, 175.
[34] Tiwari A, Rohiwal S, Suryavanshi M, Ghosh S, Pawar S. Detection of the genomic DNA of pathogenic α-proteobacterium *Ochrobactrum anthropic* via magnetic DNA enrichment using pH responsive BSA@Fe_3O_4 nanoparticles prior to in-situ PCR and electrophoretic separation. *Microchim Acta*. **2015**; DOI 10.1007/s00604-015-1710-6.
[35] Li Y, Church J, Woodhead. A. Infrared and Raman spectroscopic studies on iron oxide magnetic nano-particles and their surface modifications. *Journal of Magnetism and magnetic materials*. **2012**; 324:1543-1550.
[36] Khatiri R, Reyhani A, Mortazavi S, Hossainalipour M. Preparation and characterization of Fe_3O_4/SiO_2/APTES core-shell nanoparticles. Proceedings of the 4th International Conference on Nanostructures, Kish Island I.R. Iran. **2012**.
[37] Kulkarni S, Sawadh P, Palei P. Synthesis and Characterization of Superparamagnetic Fe_3O_4@SiO_2 Nanoparticles. *Journal of the Korean Chemical Society*. **2014**; 58.1.
[38] Ma M, Zhang Y, Yu W, Shen H-Y, Zhang H-Q, Gu N. Preparation and characterization of magnetite nanoparticles coated by amino silane. *Colloids and Surfaces A: Physicochem. Eng. Aspects*. **2003**; 212:219-226.
[39] Saif B, Wang C, Chuan D, Shuang S. Synthesis and Characterization of Fe_3O_4 coated on APTES as carriers for Morin-Anticancer Drug. *Journal of Biomaterials and Nanotechnology.* **2015**: 6; 267-275.
[40] Shrifian A, Taghi M, Nasr M, Ekramian E. Chitosan-modified superparamagnetic iron oxide nanoparticles: design, fabrication, characterization and antibacterial activity. *Chemik.* **2015**; 69, 1:19-32.
[41] Ramya R., Sudha P. N., Mahalakshmi J. Preparation and characterization of chitosan Binary Bled. *International Journal of Scientific and Research Publications*. **2012**, 2, 1.
[42] Darder M., Colilla M., Ruiz-Hitzky E. Chitosan-clay nanocomposites: application as electrochemical sensors. *Applied Clay Science.* **2005**, 28, 199-208.
[43] Chen Y.H. Thermal properties of nanocrystalline goethite, magnetite, and maghemite. *Journal of Alloys and Compounds*. **2013**. 553:194-198.
[44] Marin T, Montoya P, Arnache O, Calderon J. Influence of surface treatment on magnetic properties of FeO nanoparticles synthesized by electrochemical method. *J. Phys. Chem. ACS*. **2016**. 7. DOI: 10.1021/acs.jpcb.6b01796.
[45] Kulkarni S, Sawadh P, Palei P. Synthesis and characterization of Superparamagnetic Fe_3O_4@SiO_2 nanoparticles. *Journal of the Korean Chemical Society.* **2014**. 58; 1:100-104.
[46] Roca A, Marco J, Morales M, Serna C. Effect of Nature and Particle Size on Properties of Uniform Magnetite and Maghemite Nanoparticles. *J. Phys. Chem. C*. **2007**; 111:18577-18584.
[47] Boyer C, Whittaker M, Bulmus V, Liu J, Davis T. The design and utility of polymer-stabilized iron-oxide nanoparticles for nanomedicine applications. *NPG Asia Mater.* **2010**; 2:23-30.
[48] B. Pacakova, S. Kubickova, G. Salas, A. Mantlikova, M. Marciello, M. P. Morales, D. Niznansky and J. Vejpravova. Internal structure of magnetic nanoparticle determines magnetic response. *Nanoscale.* **2017**, DOI: 10.1039/C6NR07262C.
[49] Cortajarena A, Ortega D, Ocampo S, Gonzalez A, Couleaud P, Miranda R, Belda C, Ayuso A. Engineering Iron Oxide Nanoparticles for clinical settings. *Nanobiomedicine*. **2014**; 1:2.
[50] Qing L, Kartikowati C, Horie S, Ogi T, Iwaki T, Okuyama K. Correlation between particle size/domain structure and magnetic properties of highly crystalline Fe_3O_4 nanoparticles. *Scientific Reports*. **2017**; 7:9894.
[51] Jun-Hua W., Seung Pil K., Hong-Ling L., Sangsig K., Jae-Seon J. , Young Keun K. Sub 5 nm magnetite nanoparticles: Synthesis, microstructure, and magnetic properties. *Materials Letters.* **2007**; 61:3124–3129.
[52] Chen Y, Zhang Y. Fluorescent quantification of amino groups on silica nanoparticles surfaces. *Anal Bioanal Chem*. **2011**; 399:2503-2509.

[53] Fields R. The Rapid Determination of Amino Groups with TNBS. *Methods Enzymol*. **1972**; 25:464-8.
[54] Luna O, Gomez J, Cárdenas C, Albericio F, Marshall S, Guzmán F. Deprotection Reagents in Fmoc Solid Phase Peptide Synthesis: Moving Away from Piperidine? *Molecules.* **2016**; 21:1542.
[55] Van de Waterbeemd M, Sen T, Biagini S, Bruce I.J. Surface functionalisation of magnetic nanoparticles: quantification of surface to bulk amine density. *Micro & Nano Letters*. **2010**; 5: 282-285.
[56] Dyawanapelly S, Jagtap D, Dandekar P, Ghosh G, JainR. Assesing safety and protein interactions of surface-modified iron oxide nanoparticles for potential use in biomedical areas. *Colloids and Surfaces B: Biointerfaces*. **2017**; 154:408-420
[57] Ming Z, Xianqing Z, Sen W, Chao C, Yali C. A simple method for purification of genomic DNA from whole blood using Fe_3O_4/Au composite particles as a carrier. *Journal of Medical Colleges of PLA*. **2009**, 24:239-243.
[58] Ali A, Zafar H, Zia M, Haq I, Phull A, Ali J, Hussain A. Synthesis, characterization, applications, and challenges of iron oxide nanoparticles. *Nanotechnology, Science and Applications.* **2016**:9 49–67.
[59] Li X, Zhang J, Gu H. Adsorption and Desorption Behaviors of DNA with Magnetic Mesoporous Silica Nanoparticles. *Langmuir*. **2011**; 27: 6099-6106.
[60] Haddad Y, Xhaxhiu K, Kopel P, Hynek D, Zitka O, Adam V. The isolation of DNA by Polycharged Magnetic Particles: An Analysis of the interaction by Zeta Potential and Particle Size. *Int. J. Mol. Sci*. **2016**, 17, 550.
[61] Poly F, Chenu C, Simonet P, Rouiller J, Jocteur L. Differences between Linear Chromosomal and Supercoiled Plasmid DNA in Their Mechanism and Extent of Adsorption on Clay Minerals. *Langmuir*. **2000**; 16:1233-1238.
[62] Vinod K K (**2004**) Total Genomic DNA extraction, quality check and quantitation. In: Proceedings of the training programme on "Classical and modern plant breeding techniques - A hands on training ", Tamil Nadu Agricultural University, Coimbatore, India. Downloaded from http://kkvinod.webs.com. pp. 109-121.
[63] Shakhmaeva I, Bulatov E, Bondar O, Saifullina D, Culha M, Rizvanov A, Abdullin T. Binding and purification of plasmid DNA using multi-layered carbon nanotubes. *Journal of Biotechnology*. **2011**;152: 102–107
[64] Tanaka T, Sakai R, Kobayashi R, Hatekeyama K, Matsunaga T. Contributions of Phosphate to DNA Adsorption/Desorption Behaviors on Aminosilane-modified Nanoparticles. *Langmuir*. **2009**; 25:2956-2961.
[65] Cai P, Huang Q, Zhang X, Chen H. Adsorption of DNA on clay minerals and various colloidal particles from an Alfisol. *Soil Biology and Biochemistry*. **2006**; 38:471-476.
[66] Liu J. Adsorption of DNA onto gold nanoparticles and graphene oxide: surface science and applications. *Phys. Chem*. **2012**; 14:10485-10496.